Modern Dynamic Simulation of a Crude Oil Plant
The System's open loop response

GABRIEL RADULESCU*
Petroleum Gas University of Ploiesti, Control Engineering, Computers and Electronics Department, 39 Bucuresti Blvd., 100680, Ploiesti, Romania

A crude oil plant is a classic unit, having one main column, several sidestrippers and pumparounds. Although its steady state modeling and simulation is a well "known-and-solved" problem, only too little is known about the dynamic simulation of such a plant intimacy.The models for that exist, but the open references mention serious difficulties in building-up a dynamic model that could be appropriate for numerical integration. On the other hand, closed commercial tools for crude oil unit study are developed every day, but they limit the user to the models, parameters and state variables that the producing company is willing to provide its clients.Following a series of two other papers [1, 2], which present in detail the problem of a crude oil plant modeling and dynamic simulation, this work makes a step ahead. An open-loop unit detailed response is given and analyzed, and also interesting features (like unit inverse response) are observed here, denoting a good agreement with plant experimental data.

Keywords: crude oil plant, dynamic simulation, open-loop behaviour.

The crude oil unit, which is a part of the Atmospheric and Vacuum Distillation plant, is the first important processing unit in any refinery. Due to its position, its high complexity and the fact that this is one of the most energy consumption plants, it is very important to have powerful instruments to intimately study it. In the recent past, a modern and dedicated software simulator, focused on the dynamic behavior of this multi-component distillation process, was extensively presented in [1,-3]. Together with the simulator itself, an original mathematical modeling approach for the process was identified, with an appropriate method to solve it.

After many years of experimentation, involving the model tuning and simulator setup, this paper presents in detail the results obtained when simulating the plant open-loop dynamic behavior, having a very good agreement with experimental data.

The plant structure and simulator representation

Figure 1 presents the crude oil plant structure, identical to those referred in [1-3], together with some important operating data (significant temperatures and flowrates in important positions).

As shown in figure 1, the plant consists in one main column (COL) with two pumparounds (PA1 and PA2) and four sidedraws to the sidestrippers (SS). The main feed is

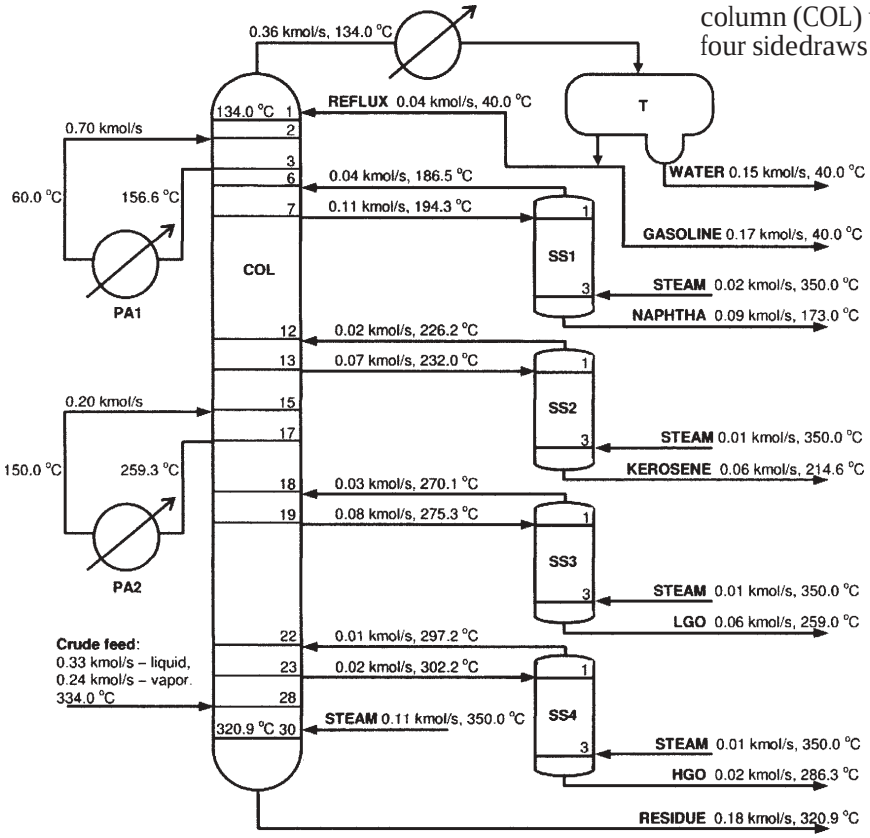

Fig. 1. Crude oil unit structure.

* email: gabriel.radulescu@upg-ploiesti.ro; Tel.: 0722779911

Feed phase	mixt (liquid + vapor)									
Feed type	dry fraction (does not contain water)									
Total flowrate	0.570 kmol/s									
Temperature	334.000 ^{0}C									
Pressure	2.400 bar									
Liquid phase flowrate	0.240 kmol/s									
Molecular weight liquid phase	434.028 kg/kmol									
Liquid phase caloric capacity	0.703 kcal/kg·^{0}C									
Liquid phase density (at feed temperature)	735.310 kg/m^3									
Vapor phase flowrate	0.330 kmol/s									
Molecular weight vapor phase	162.928 kg/kmol									
Vapor phase caloric capacity	0.639 kcal/kg·^{0}C									
Vapor phase density (at feed temperature)	8.175 kg/m^3									
TBP initial data (liquid feed)	%distilled	0	10	20	30	40	50	60	70	80
	T (^{0}C)	94	141	202	254	306	368	427	504	580

Table 1
THE MAIN FEED STREAM DATA

	Steam to COL	**Steam to SS1**	**Steam to SS2**	**Steam to SS3**	**Steam to SS4**
Feed type	Dry fraction (does not contain water)				
Flowrate	0.101 kmol/s	0.016 kmol/s	0.012 kmol/s	0.014 kmol/s	0.005 kmol/s
Temperature	350.000 ^{0}C				
Pressure	5.000 bar				
Molar weight	18.015 kg/kmol				
Enthalpy	756.118 kcal/kg				
Calorin capacity	0.492 kcal/kg·^{0}C				
Density	1.753 kg/m^3				

Table 2
THE STEAM STREAMS DATA

	Upper pumparound (PA1)		**Lower pumparound (PA2)**	
Input temperature (TIN)	156.000	^{0}C	259.300	^{0}C
Output temperature (TOUT)	60.000	^{0}C	150.000	^{0}C
Input caloric flow (Q_{IN})	7405.555	kcal/s	6007.778	kcal/s
Output caloric flow (Q_{OUT})	2520.555	kcal/s	3085.278	kcal/s
Product flowrate (FIN)	0.698	kmol/s	0.202	kmol/s

Table 3
THE ASSOCIATED DATA FOR PA1 AND PA2 PUMPAROUNDS

the crude oil, while the others are steam (considered pure water). The top vapor is totally condensed and stored in a tank (T) where the water is decanted and taken out of the system. Part of the top product turns back at the main column top as external reflux, the rest being the plant top product (gasoline). From the sidestrippers, the side products are withdrawn (naphtha, kerosene, light gas oil – LGO – and heavy gas oil – HGO). The bottom product is the crude oil plant residue.

The main feed data are presented in table 1.

It is important to mention that all material streams, including the crude oil feed, were divided into $NC = 37$ pseudo-components (36 hydrocarbon type, one component the added water), in order to represent the true-boiling-point (TBP) curve.

Regarding the steam, table 2 shows the main data associated to the 5 streams. At the same time, table 3 depicts the characteristics of the two pumparound streams.

In [1- 3], some considerations regarding the problem of representing this huge plant inside the simulator were presented in detail. Also, the same problems were shown in [4, 5]. To simulate the dynamics of the crude oil unit means to integrate its mathematical model equations, having adequate routines for that. We used DIVA (Dynamische Simulation Verfahrenstechnischer Anlagen), developed at the Stuttgart University [6-11], a versatile and powerful software oriented on dynamic simulations for industrial plants. Inside DIVA, the model shown in detail in [1-3] was implemented, primarily resulting a total number of 9125 equations, with 1598 differential and 7527 algebraic equations. Together with this, 5 equations were added to implement the bottom column and sidestrippers level controllers, imposing the residue flowrate (for main column) and sidedraws from the column flowrates (for sidestrippers) to be controlled variables [3]. The reason why the liquid level is considered (perfectly) controlled in all these points is that all material streams have to be balanced, otherwise (with variable liquid phase accumulation) the whole system cannot reach a true steady state.

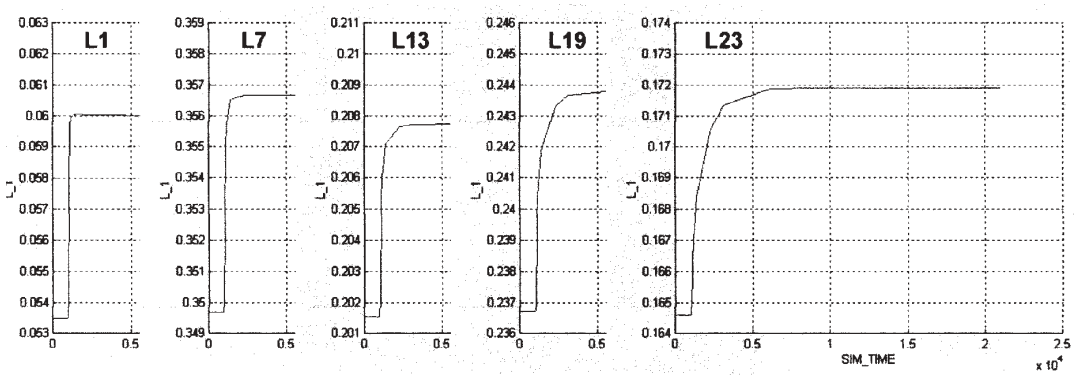

Fig. 2. Plant open-loop response for a 13% increase in reflux ratio. Internal reflux from trays 1, 7, 13, 19 and 23, in [kmol/s], are depicted. The simulation time is expressed in [s× 10^4]

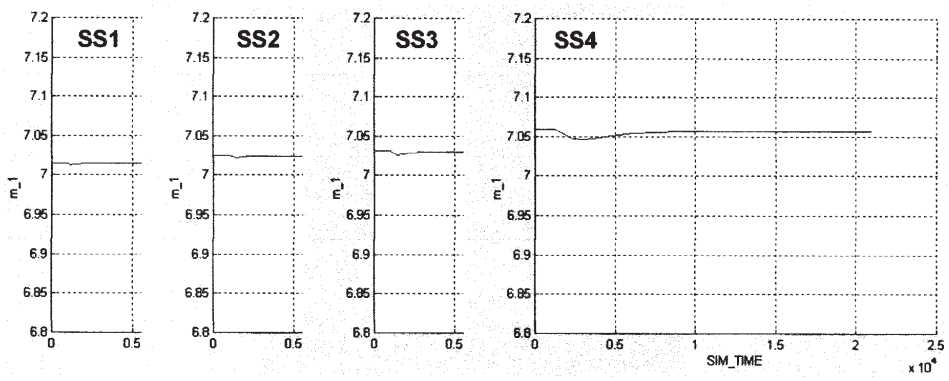

Fig. 3. Plant open-loop response for a 13% increase in reflux ratio. Sidestrippers bottom liquid accumulation, in [kmol], are shown. The simulation time is expressed in [s × 10^4].

Finally, there is a need to validate this model implementation. As shown in [1, 2], for such a huge internal representation we have to keep in mind that all analytical methods cannot be applied practically. On the other hand, only a significant number of simulation scenarios and a strict comparison (qualitative/quantitative) with the real plant data can give us the model and simulator validity flavor, as proven in [3]. In fact, the model together with its simulator implementation were tested along the years, so now the author (and not only) is definitively positive when deciding on their validity.

Plant open-loop simulations

Keeping in mind that the final aim of the work would be to integrate all control systems and to simulate the crude oil unit in this new structure, the first step would be to simulate the "open-loop" system, meaning there are no supplementary equipment on the plant, except the five level controllers mentioned above. Such a methodology, starting from the open-loop plant structure, always offers an important set of data like system validity, inputs sensitivity and it (maybe) shows some intricate plant behavior, also known from the real operating experience.

In this chapter, in order to keep a reasonable work size, the author selected a limited number of significant simulation results by firstly modifying the reflux ratio in the main column and, secondly, by changing the kerosene flowrate at the SS2 sidestripper.

System response when changing the reflux ratio

A change in the reflux ratio proves to be a very interesting experiment for the main column, judging from the severe drift that affects its internal hydraulic regime. All these simulations were performed with a ratio increase from 0.23 to 0.26 (13% relatively).

Figure 2 shows the flowrates of liquid leaving the first column tray (L_1) and the withdrawn trays for products handled by the sidestrippers (L_7, L_{13}, L_{19} and L_{23}).

While the L_1 instantaneously steps up, there is an increasing delay when descending in the column; the maximum value is for the 23rd tray (about 5000 s). The changes into the internal reflux are not caused only by the external one, but also by slightly modifying the tray composition, the liquid/vapor ratios, while the stripping steam to the main column remains unchanged. The changes in L_1, L_7, L_{13}, L_{19} and L_{23} flowrates have practically the same amplitude, so the internal reflux seems to linearly change [3].

But this increase seems not to have the same impact to the SS1, SS2, SS3 and SS4 sidestrippers bottom liquid accumulation, as proven by figure 3.

This is absolutely normal, because the naphtha, kerosene, LGO and HGO flowrates are kept constant. Nevertheless, very small changes appear, due to the fact that small composition changes for stripped liquids leads to the same liquid/vapor ratio changes on sidestrippers trays.

The internal reflux increase produces the heavy components' migration to the column bottom, so the light components presence in the withdrawn phases from the main column increases. By keeping constant the steam to SS1, SS2, SS3 and SS4, a light vapor phase increases at these sidestrippers' top, leading to changes in level controllers output in order to satisfy the material balances (fig. 4) [3].

The changes in the external reflux lead to temperature modifications on trays T_1, T_7, T_{13}, T_{19} and T_{23}. Figure 5 shows their decreasing, which combines two causes.

First, there is a large presence of a cooler liquid phase on trays (the reflux having a temperature of 40^0C, in comparison with 134^0C which is the temperature on tray 1). Secondly, as shown above, the presence of lighter components on these trays increases (as they have lower boiling points). Obviously, the composition changes (including its inner delay) have the major influence in these temperature values [3].

Figure 6 shows the external reflux influence on the gasoline, naphtha, kerosene, LGO and HGO end boiling points (EP). The heavier components' migration to the column base decreases all these product values.

It has to be shown that the EP's dynamics is quite the same for successive products, meaning that the slow mass

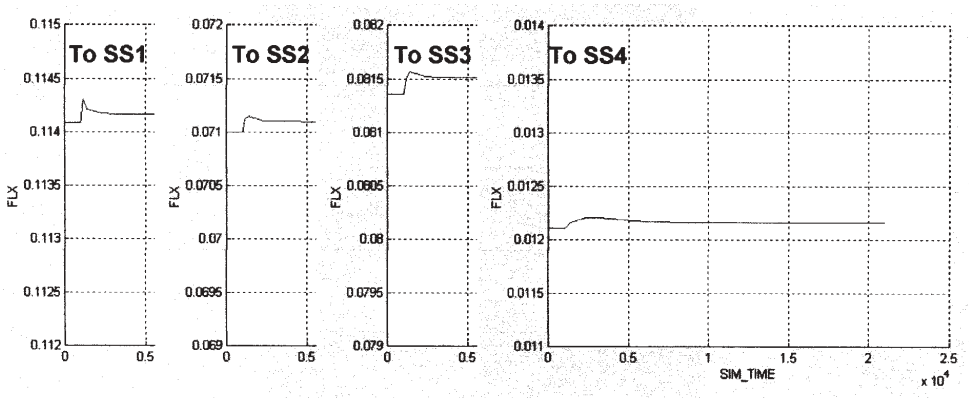

Fig. 4. Plant open-loop response for a 13% increase in reflux ratio. Liquid sidedraws to SS1, SS2, SS3 and SS4, in [kmol/s], are presented. The simulation time is expressed in [s × 10^4].

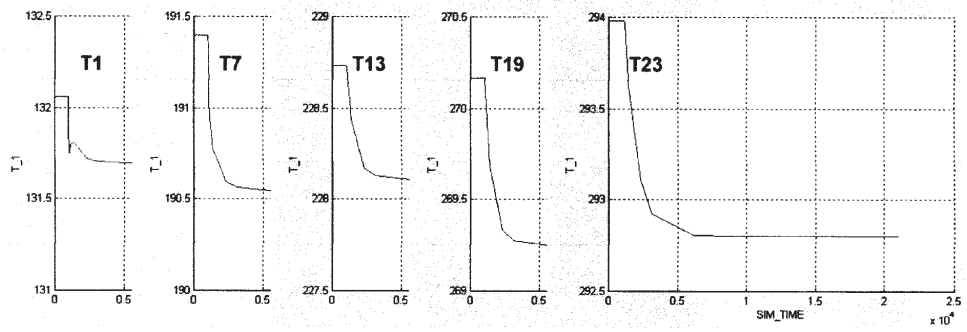

Fig. 5. Plant open-loop response for a 13% increase in reflux ratio. Trays 1, 7, 13, 19 and 23 temperatures, in [^{0}C], are shown. The simulation time is expressed in [s × 10^4].

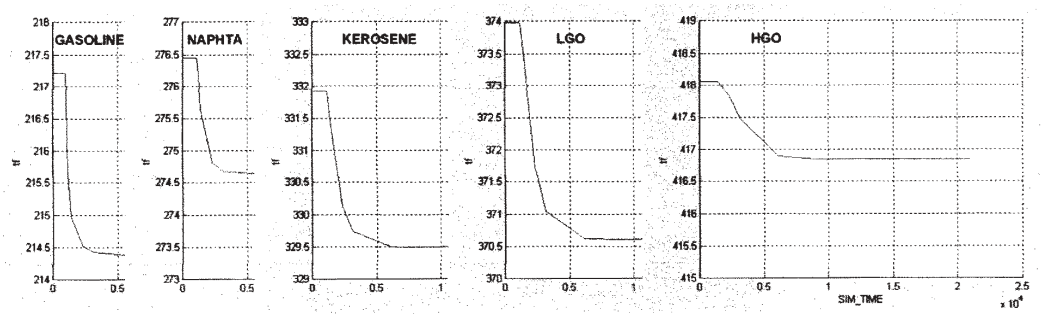

Fig. 6. Plant open-loop response for a 13% increase in reflux ratio. The gasoline, naphtha, kerosene, LGO and HGO EP, in [^{0}C], are depicted. The simulation time is expressed in [s × 10^4].

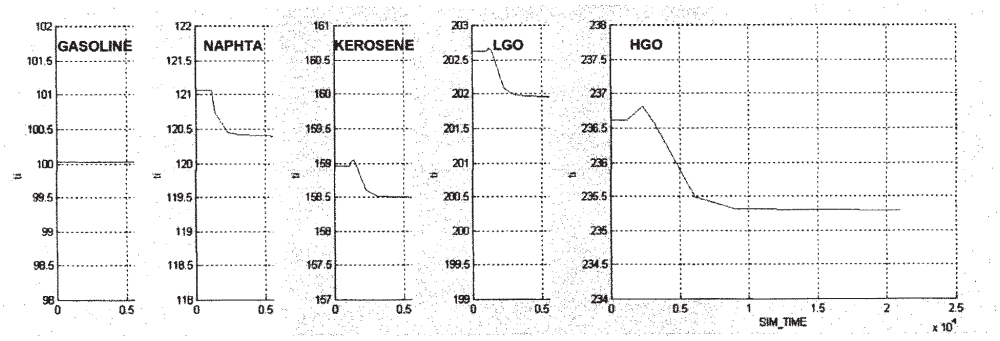

Fig. 7. Plant open-loop response for a 13% increase in reflux ratio. The gasoline, naphtha, kerosene, LGO and HGO SP, in [^{0}C], are depicted. The simulation time is expressed in [s × 10^4].

transfer process between the liquid and vapor phase takes place simultaneously into the whole column.

The external reflux change has a lower influence on the crude oil unit products start boiling points (SP), as depicted by figure 7.

For the gasoline, its SP (a constant value of 100.025^{0}C) is given only by the lightest pseudo-component into the system, this being dependent only by the crude oil feed quality disturbances. On the other hand, the increasing presence of lighter components on column trays has a slight influence on side products SP (between 0.5^{0}C and 1.2^{0}C, in comparison to 3…3.5^{0}C for EP). But it is very interesting to reveal also the system's *inverse response* for kerosene, LGO and HGO products (a short initial increase in SP values, followed by a normal decreasing), proving that the mathematical model follow in detail the real system [3].

System response when changing the kerosene flowrate

By modifying a side product flowrate, the biggest influence is on the product composition (it mainly changing the product EP). At the same time, the level controller for the implied stripper bottom liquid accumulation modifies its output, by changing the column liquid withdrawn, leading to an internal reflux changing below the column extraction tray.

Figure 8 depicts how a 10% increase in kerosene flowrate makes the column internal reflux to decrease by about 0.015 kmol/s below the 13th tray having no influence on the column upper part (trays 1 and 7).

This internal reflux changing is a consequence of level controller action, which increases the liquid withdrawn to SS2 in order to keep a constant level at the sidestripper bottom, as figure 9 depicts.

As the control algorithm was only a proportional one, it is to expect a permanent drift (comparing with the setpoint) in kerosene level at the SS2, as shown in figure 10. However, the level error is minor (as long as the total liquid accumulation lowers with 1.42%), so a "perfect" level controller for SS2 bottom still may be taken into account. At the same time, figure 10 shows the SS1, SS3 and SS4 level controllers working perfectly [3].

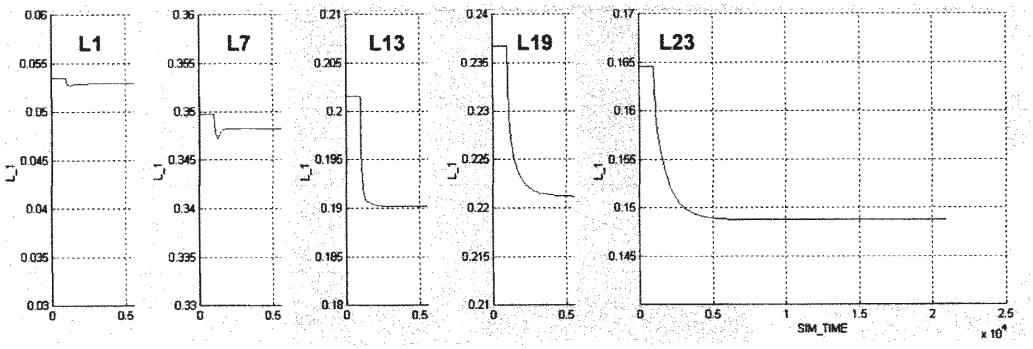

Fig. 8. Plant open-loop response for a 10% increase in kerosene flowrate. Internal reflux from trays 1, 7, 13, 19 and 23, in [kmol/s], are depicted. The simulation time is expressed in [s × 10^4]

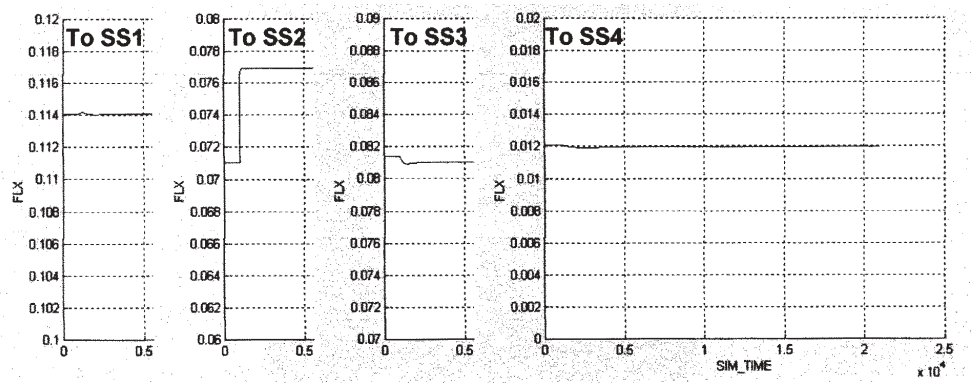

Fig. 9. Plant open-loop response for a 10% increase in kerosene flowrate. Liquid sidedraws to SS1, SS2, SS3 and SS4, in [kmol/s], are presented. The simulation time is expressed in [s × 10^4]

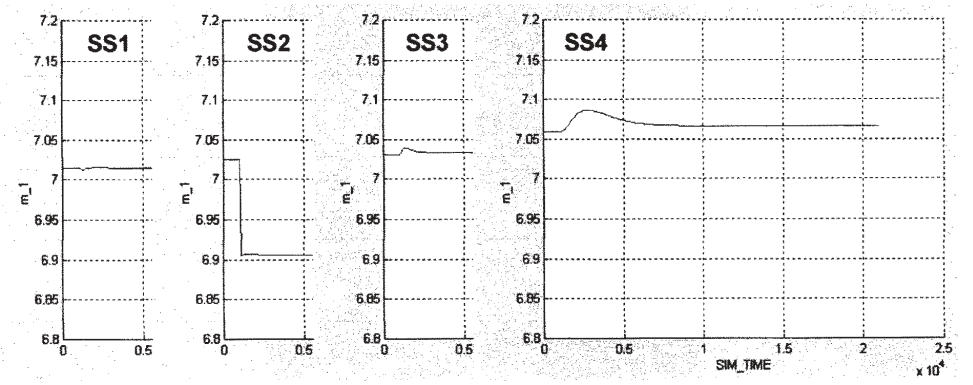

Fig. 10. Plant open-loop response for a 10% increase in kerosene flowrate. Liquid accumulation for SS1, SS2, SS3 and SS4 bottom, in [kmol], are presented. The simulation time is expressed in [s × 10^4].

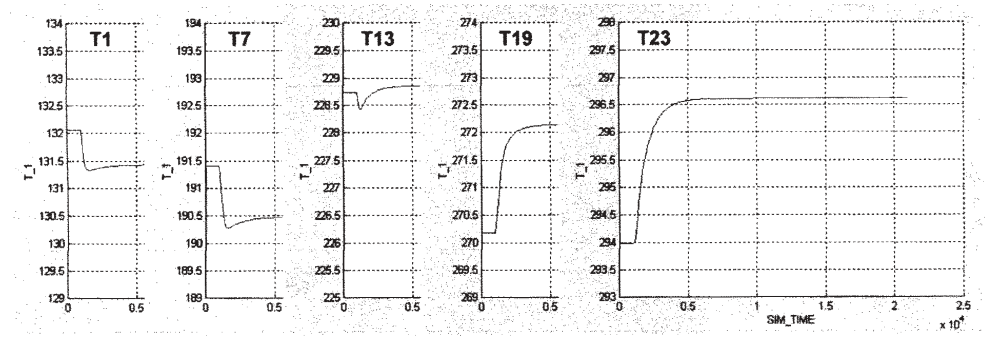

Fig. 11. Plant open-loop response for a 10% increase in kerosene flowrate. Trays 1, 7, 13, 19 and 23 temperatures, in [^{0}C], are shown. The simulation time is expressed in [s × 10^4].

Figure 11 depicts how this increase in kerosene flowrate influences the column temperatures. The internal reflux flowrate, having a lower temperature, reduces under the 13th tray. Simultaneously, on the influenced column zone the heavier liquid components are more present, leading to an increasing temperature on trays 19 and 23 (with no influence on extracting tray 13).

At the same time, the complex influences into the system produce a temperature lowering on trays 1 (0.5^{0}C) and 7 (1^{0}C), due to liquid/vapor ratio changing on column trays. Also, the heavier components increasing presence at the column lower part makes the lighter components migrate to the upper part, leading to the same temperature changing direction [3].

As the internal reflux lowers, all the column sidedraws below the 13th tray are rich in heavier components. As a consequence, all stripped products (coming below the 13 tray) have bigger values for their EP, as figure 12 presents.

The kerosene, LGO and HGO EP's increase, respectively, by 2.5, 3.5 and 3^{0}C, but the effect is strictly unidirectional (the naphtha EP increasing by 0.5^{0}C, while the gasoline EP decreases by about 2^{0}C).

It seems that the internal reflux changing influences more the products SP, except the gasoline, as shown in figure 13. The naphtha and kerosene products SP's decrease with 1, respectively 1.5^{0}C, while the LGO and HGO SP's increase with 1.5 and 3^{0}C.

The crude oil plant acts in the same way like in the previous experiment, showing an inverse response for LGO and HGO SP's when the kerosene flowrate increases with 10%, the fact being proven from the real unit operation [3].

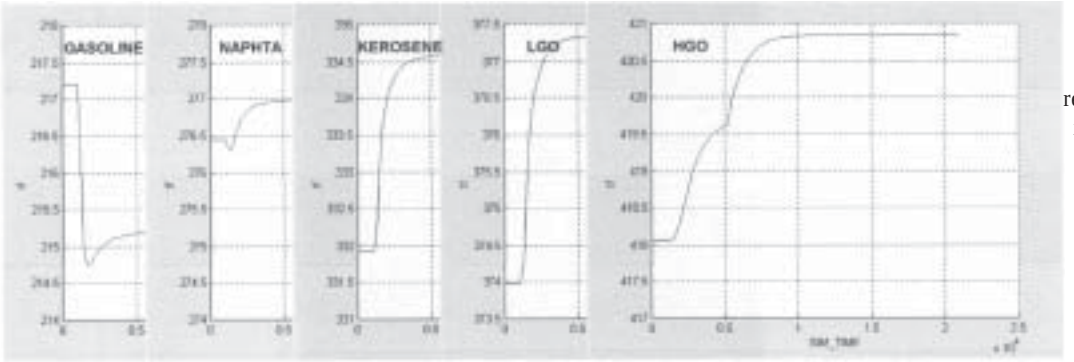

Fig. 12. Plant open-loop response for a 10% increase in kerosene flowrate. The gasoline, naphtha, kerosene, LGO and HGO EP, in [^{0}C], are depicted. The simulation time is expressed in [s × 10^4].

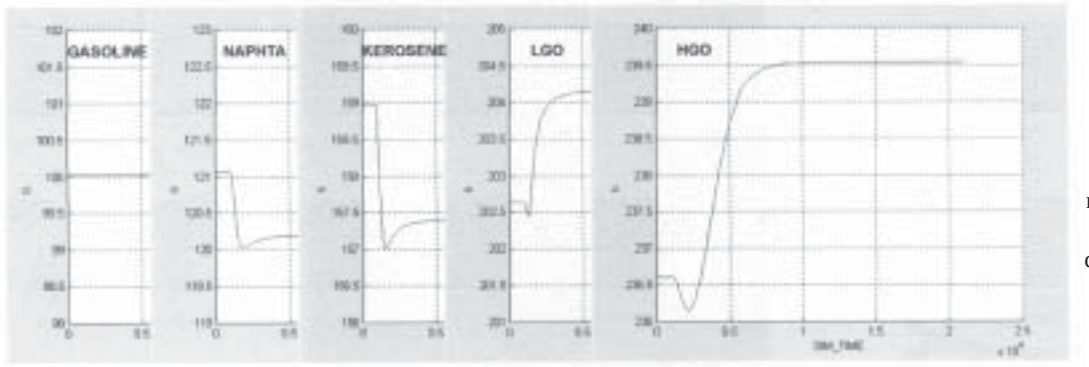

Fig. 13. Plant open-loop response for a 10% increase in kerosene flowrate. The gasoline, naphtha, kerosene, LGO and HGO SP, in [^{0}C], are depicted. The simulation time is expressed in [s × 10^4]

Conclusions

As an overall conclusion, the crude oil unit open-loop response (when using our proposed simulator) is remarkably close to the real system, respecting the qualitative and quantitative plant behavior. The given response was analyzed in detail, and also interesting features (like unit inverse response) are observed here, showing a good fit with plant experimental data. This is why future experiments may be planned, especially in the field of advanced process operation and plant control.

References

1.RADULESCU, G., Rev. Chim. (Bucharest), **58**, no. 2, 2007, p. 239.
2.RADULESCU, G., PARASCHIV, N., KIENLE, Rev. Chim. (Bucharest), **58**, no. 3, 2007, p. 349
3.RADULESCU, G., Reglarea evoluatã a procesului de distilare atmosfericã, Editura Universitãii Petrol-Gaze din Ploiesti, Ploiesti, 2015.
4.RADULESCU, G., PARASCHIV, N., MIHALACHE, S., Rev. Chim. (Bucharest), **64**, no. 9, 2013, p. 1043
5.RADULESCU, G., MIHALACHE, S. F., POPESCU, M., Rev. Chim. (Bucharest), **65**, no. 6, 2014, p. 718
6.MARQUARDT, W., HOLL, P., GILLES, E. D., Proc. of the IIIrd World Congress of Chemical Engineering, Tokyo, 1986, p. 687.
7.GILLES, E. D., HOLL, P., MARQUARDT, W., MAHLER, R., SCHNEIDER, H., BRINKMANN, K., WILL, K. H., Automatisierungstechnische Praxis, **32**, 1990, p. 343.
8.MANGOLD, M., KIENLE, A., MOHL, K, D., GILLES, E. D., Chem. Engng. Sci., **55**, 2000, p. 441.
9.MARQUARDT, W., HOLL, P., BUTZ, D., GILLES, E. D., Chem. Engng. Tech., **10**, 1987, p. 164.
10.KRONER, A., HOLL, P., MARQUARDT, W., GILLES, E. D., Comput. Chem. Engng., **14**, 1990, p. 1289.
11.TRANKLE, F., GERSTLAUER, A., ZEITZ, M., GILLES, E. D., Comput. Chem. Engng. (Suppl.), **21**, 1997, p. 841.

Manuscript received: 28.07.2015